

# On cosmological properties of black-hole hair in linearly coupled scalar–Gauss–Bonnet theory

Dražen Glavan <sup>1,\*</sup> and Darío Jaramillo-Garrido <sup>2,†</sup>

<sup>1</sup>*CEICO, Institute of Physics of the Czech Academy of Sciences,  
Na Slovance 1999/2, 182 21 Prague 8, Czech Republic*

<sup>2</sup>*Departamento de Física Teórica and Instituto de Física de Partículas y del Cosmos (IPARCOS-UCM),  
Universidad Complutense de Madrid, E-28040 Madrid, Spain*

We investigate the superhorizon behavior of scalar hair sourced by black holes in de Sitter spacetime in the linearly coupled shift-symmetric scalar–Gauss–Bonnet theory. Working in the test-field regime, we show that this hair exhibits both temporal and spatial growth on superhorizon scales. This growth is not a special consequence of the black hole, but instead follows from the dynamics of a minimally coupled massless scalar field in expanding de Sitter spacetime. Moreover, it is not even specific to black holes, but also arises for a point scalar charge in de Sitter, indicating that a scalarized black hole acts effectively as a localized subhorizon source of scalar perturbations. Backreaction, when important, first arises on subhorizon scales and does not by itself eliminate the superhorizon profile. The time-dependent scalar hair also carries a steady outward energy flux, which frames the test-field regime as a transient, and helps explain the difficulties encountered in attempts to construct self-consistent static solutions.

## I. INTRODUCTION

Black holes in general relativity obey strong no-hair results [1], which in particular exclude nontrivial profiles of a canonical scalar field for asymptotically flat solutions under standard assumptions. Analogous no-hair results were established for static, spherically symmetric black holes in shift-symmetric Horndeski theories [2]. However, these results do not apply to all shift-symmetric Horndeski theories, and an exception was identified in [3] for a particular subclass.

This exception arises when the scalar field couples linearly to the Gauss–Bonnet invariant. In that case, the scalar-field equation acquires a source term even in vacuum, so the assumptions underlying the no-hair results no longer apply (see also [4] for a detailed study of coupling functions which evade the no-hair theorems). Explicit asymptotically flat hairy black-hole solutions in this linearly coupled shift-symmetric theory were constructed perturbatively in the test-field regime in [3], and numerically as self-consistent solutions in [5]. The resulting hair is secondary [6, 7], in the sense that it is not associated with an independent asymptotic charge, but is instead fixed by the black-hole parameters and the Gauss–Bonnet coupling.

For sufficiently small black-hole masses, the test-field approximation breaks down because the scalar backreaction can no longer be neglected, and the full coupled field equations must be solved self-consistently. The numerical analysis of [5] showed that regular black-hole solutions in this theory exist only above a minimum mass. For the self-consistent solutions that were constructed, deviations from the Schwarzschild geometry remain com-

paratively small away from the immediate vicinity of the black hole.

Subsequent work showed that this hair can form dynamically from regular initial data, and also investigated the stability properties of the corresponding black-hole solutions [8, 9]. This strengthens the interpretation of the hairy solutions as physically relevant configurations, rather than merely formal stationary solutions. Moreover, the generalization to the more physically realistic Kerr black holes was also considered [10].

The situation becomes more subtle once one asks whether these hairy black-hole solutions can be embedded consistently in a cosmological spacetime. Earlier numerical attempts to construct static scalarized black holes with de Sitter asymptotics found no solutions [11, 12]; see also [13]. Recent work [14] proposed that this failure can be traced to the cosmological horizon, which obstructs static scalar hair for a spherically symmetric black hole in an expanding de Sitter background.

In Ref. [14], the scalar field was allowed to depend linearly on time as well as radius, while still yielding a stationary energy-momentum tensor because of shift symmetry. An explicit solution for the scalar hair was constructed in static coordinates in the test field approximation. It shows scalar hair that decays very slowly with distance from the black hole, and extending all the way to the cosmological horizons where it does not match the expected cosmologically rolling homogeneous and isotropic solution. The question of whether such a solution is physically reasonable was raised since it would suggest that a local black-hole configuration can qualitatively alter the large-distance cosmological behavior of the spacetime. It then becomes important to understand the physical origin of this unexpected feature.

Here we revisit the properties of black-hole scalar hair on cosmological scales. We show that its large-distance profile is controlled not by the local black-hole structure

\* email: [glavan@fzu.cz](mailto:glavan@fzu.cz)

† email: [djaramil@ucm.es](mailto:djaramil@ucm.es)

or by the scalarization mechanism specific to the linearly coupled scalar–Gauss–Bonnet theory, but by the cosmological dynamics of a minimally coupled massless scalar field. The same dynamics underlies the generation of nearly scale-invariant superhorizon scalar perturbations during inflation [15].

Moreover, this profile is not unique to black holes. It was obtained previously for a point scalar charge in de Sitter space in [16], and later rederived in [17, 18]. This indicates that, on cosmological scales, a black hole is effectively indistinguishable, as a source of the scalar field, from any other static, spherically symmetric localized scalar charge. At those scales, the information about the source enters only through the overall amplitude of the profile, which is fixed locally by the black-hole mass and the Gauss–Bonnet coupling.

From a cosmological perspective, a scalarized black hole acts as a localized source of scalar perturbations well inside the cosmological horizon. As the universe expands, these perturbations are stretched to superhorizon scales and amplified, giving rise to a nearly scale-invariant spectrum. The resulting picture is simple: the black hole seeds the hair locally, while cosmological expansion determines its asymptotic form. We derive this picture explicitly for a point source in de Sitter, and then show that the scalar profile of a black hole in Schwarzschild–de Sitter spacetime follows the same asymptotic pattern, with both systems also exhibiting an outward energy flux associated with the time-dependent scalar configuration.

To disentangle the different ingredients of the problem, we consider three complementary settings: the Schwarzschild spacetime in Sec. III, a scalar point source in de Sitter spacetime in Sec. IV, and the Schwarzschild–de Sitter spacetime in Sec. V. Each example is analyzed in the test-field approximation, with particular attention to the regime in which scalar backreaction becomes important. We find that the first breakdown of the test-field description occurs on subhorizon scales. Any reliable conclusion about the cosmological-scale scalar-hair profile therefore requires understanding the nonlinear dynamics near the black hole.

## II. PRELIMINARIES

In this section we collect the basic equations of the theory and introduce the invariant diagnostic that will be used throughout the paper to estimate when the test-field approximation is expected to break down.

We consider the linearly coupled shift-symmetric scalar–Gauss–Bonnet (sGB) theory, with action

$$S[g_{\mu\nu}, \Phi] = \int d^4x \sqrt{-g} \left[ \frac{M_{\text{p}}^2}{2} (R - 2\Lambda) + X + \alpha \Phi \mathcal{G} \right], \quad (1)$$

where  $X = -\frac{1}{2}g^{\mu\nu} \partial_\mu \Phi \partial_\nu \Phi$  is the scalar kinetic term,  $\Lambda$  is the cosmological constant,  $M_{\text{p}} = 1/\sqrt{8\pi G_{\text{N}}}$  is the reduced Planck mass, and  $\mathcal{G} = R^2 - 4R^{\mu\nu}R_{\mu\nu} + R^{\mu\nu\rho\sigma}R_{\mu\nu\rho\sigma}$  is the Gauss–Bonnet invariant.

The scalar equation of motion is

$$\square \Phi = \frac{1}{\sqrt{-g}} \partial_\mu (\sqrt{-g} g^{\mu\nu} \partial_\nu \Phi) = -\alpha \mathcal{G}, \quad (2)$$

while the energy-momentum tensor is

$$\mathcal{T}_{\mu\nu} = \nabla_\mu \Phi \nabla_\nu \Phi + X g_{\mu\nu} - 8\alpha P_{\mu\nu\rho\sigma} \nabla^\rho \nabla^\sigma \Phi, \quad (3)$$

where  $P_{\mu\nu\rho\sigma} = R_{\mu\nu\rho\sigma} - 4g_{\mu[\rho}R_{\sigma][\nu} + Rg_{\mu[\rho}g_{\sigma]\nu}$  is proportional to the double-dual of the Riemann tensor,  $P_{\mu\nu\rho\sigma} = (-1) \times \frac{1}{4} \epsilon_{\mu\nu\alpha\beta} \epsilon_{\rho\sigma\gamma\delta} R^{\alpha\beta\gamma\delta}$ . We will frequently use the trace of the energy-momentum tensor,

$$\mathcal{T} = 2X + 8\alpha G_{\mu\nu} \nabla^\mu \nabla^\nu \Phi, \quad (4)$$

where  $G_{\mu\nu} = R_{\mu\nu} - \frac{1}{2}g_{\mu\nu}R$  is the Einstein tensor.

Since we will consider the Schwarzschild, de Sitter, and Schwarzschild–de Sitter spacetimes, it is useful to introduce a simple invariant estimate of the size of scalar backreaction. We do so by comparing the trace of the scalar energy-momentum tensor to the local curvature scale set by the Kretschmann invariant,

$$\mathcal{K} = R^{\mu\nu\rho\sigma} R_{\mu\nu\rho\sigma}. \quad (5)$$

Accordingly, we define

$$b \equiv \left| \frac{\mathcal{T}}{M_{\text{p}}^2 \sqrt{\mathcal{K}}} \right|. \quad (6)$$

This quantity does not replace a full solution of the coupled field equations, but it provides a convenient invariant diagnostic for identifying the regime in which the test-field approximation is expected to fail.

## III. SCHWARZSCHILD SPACETIME

We begin with the Schwarzschild spacetime, summarizing the derivation of [3] in order to collect the results that will be useful later and to establish the picture that we expect to remain valid on subhorizon scales in the cosmological setting, in the regime where the two horizons are widely separated that will be considered in the following sections.

The line element in Schwarzschild coordinates is

$$ds^2 = -f(r) d\tau^2 + \frac{dr^2}{f(r)} + r^2 d\Omega^2. \quad (7)$$

where  $f(r) = 1 - r_{\text{s}}/r$ , and where  $r_{\text{s}} = 2GM$  is the Schwarzschild radius related to the black hole mass  $M$ . In this spacetime, one has  $\mathcal{G} = \mathcal{K} = 12r_{\text{s}}^2/r^6$ . Assuming a radially dependent scalar profile,  $\Phi = \Phi(r)$ , the equation of motion (2) reduces to

$$\frac{d}{dr} \left( r^2 f(r) \frac{d\Phi}{dr} \right) = -\frac{12\alpha r_{\text{s}}^2}{r^4}. \quad (8)$$

Integrating once gives

$$\frac{d\Phi}{dr} = \frac{4\alpha r_s^2}{r^5 f(r)} - \frac{\mathcal{C}}{r^2 f(r)}, \quad (9)$$

where  $\mathcal{C}$  is an integration constant. Requiring the scalar gradient to remain finite at the black-hole horizon fixes it to

$$\mathcal{C} = \frac{4\alpha}{r_s}. \quad (10)$$

This shows that the scalar hair is secondary: the integration constant is not an independent scalar charge, but is instead fixed by the coupling constant and the black-hole mass.

Consequently, the scalar hair profile, up to an irrelevant integration constant, is

$$\Phi(r) = \frac{4\alpha}{r_s r} \left[ 1 + \frac{r_s}{2r} + \frac{r_s^2}{3r^2} \right]. \quad (11)$$

An important point is that this profile remains finite at the horizon even in Schwarzschild coordinates. Thus, in this particular case there is no need to invoke horizon-regular coordinates in order to establish regularity of the scalar field. Nevertheless, it will be useful to introduce such coordinates already here, since they provide a natural basis for comparison with the more complicated cases to follow. A convenient choice is given by Painlevé–Gullstrand coordinates [19], obtained from Schwarzschild coordinates through the time transformation

$$\tau = t + \int \frac{dr}{f(r)} \sqrt{1-f(r)}. \quad (12)$$

This puts the line element (7) in the manifestly non-singular form

$$ds^2 = -dt^2 + \left( dr - \sqrt{1-f(r)} dt \right)^2 + r^2 d\Omega^2. \quad (13)$$

Because the scalar hair profile (11) is static, it is unchanged by this coordinate transformation and remains a function of  $r$  only.

Having obtained the scalar hair profile, we can compute the trace of the energy-momentum tensor. In the Schwarzschild background it receives no direct contribution from the Gauss–Bonnet coupling, but only from the scalar kinetic term,

$$\mathcal{T} = -\frac{16\alpha^2}{r_s^2} \frac{f(1-f)^4}{r_s^4} \left[ f^2 + 3(1-f) \right]^2. \quad (14)$$

This should be compared with the Kretschmann invariant,

$$\mathcal{K} = \frac{12r_s^2}{r^6} \quad (15)$$

which sets the local curvature scale of the Schwarzschild geometry. The corresponding backreaction measure (5) is therefore

$$b = \frac{16\alpha^2}{M_{\text{P}}^2 r_s^4} \frac{f(1-f)}{\sqrt{12}} \left[ f^2 + 3(1-f) \right]^2. \quad (16)$$

Its behavior is shown in Fig. 1. The backreaction becomes appreciable first close to the black-hole horizon, while remaining small both at the horizon and at large distances.

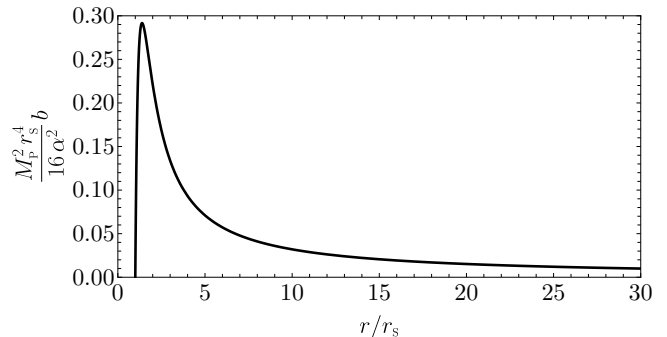


**Fig. 1.** Strength of the backreaction of the scalar field on the Schwarzschild background. The backreaction first becomes important close to the black hole.

An important consequence of Eq. (16) is that the backreaction becomes stronger for smaller black holes. Since the backreaction measure scales inversely with the fourth power of the Schwarzschild radius, decreasing  $r_s$  drives the system more quickly toward the breakdown of the test-field approximation. This is precisely why solving the full coupled field equations becomes necessary for sufficiently small black holes. Such self-consistent solutions were constructed numerically in [5], where this behavior was shown to imply a minimum allowed black-hole mass in the theory.

#### IV. POINT SOURCE IN DE SITTER SPACETIME

A point scalar charge in de Sitter spacetime provides the simplest setting in which to isolate the cosmological behavior of a localized scalar source, without the additional near-source structure associated with a black hole. It therefore allows us to distinguish the generic cosmological properties of the large-distance scalar profile from those tied specifically to black-hole scalarization.

We adopt conformal cosmological coordinates for expanding de Sitter spacetime,

$$ds^2 = a^2(\eta) (-d\eta^2 + d\vec{x}^2), \quad (17)$$

$\eta \in (-\infty, 0)$  is conformal time,  $a(\eta) = -1/(H\eta)$  is the scale factor, and  $H = \sqrt{\Lambda/3}$  is the Hubble rate.

We consider the scalar theory (1) on this background. The scalar is sourced both by the Gauss–Bonnet invariant of de Sitter spacetime,  $\mathcal{G} = 24H^4$ , and by a scalar point charge placed at the origin of the comoving coordinate

system,<sup>1</sup>

$$\square\Phi = -\frac{1}{a^2} \left[ \partial_\eta^2 + 2aH\partial_\eta - \nabla^2 \right] \Phi = -24\alpha H^4 - \frac{4\pi\beta\delta^3(\vec{x})}{a^3}. \quad (18)$$

Because the equation of motion is linear, the full solution can be decomposed into the homogeneous part sourced by the de Sitter background and the part sourced by the point charge. The former is removed by the time-dependent shift

$$\Phi(\eta, x) = 8\alpha H^2 \ln(a) + \phi(\eta, x), \quad (19)$$

where  $x = \|\vec{x}\|$ , so that the remaining field satisfies

$$\left[ \partial_\eta^2 + 2aH\partial_\eta - \nabla^2 \right] \phi = \frac{4\pi\beta\delta^3(\vec{x})}{a}. \quad (20)$$

This is precisely the equation studied in [16–18] for a minimally coupled massless scalar field sourced by a point charge in de Sitter spacetime.<sup>2</sup>

The solution to Eq. (20) was obtained in [16–18] and reads

$$\phi(\eta, x) = \frac{\beta}{ax} + \beta H \ln\left(\frac{a}{1+aHx}\right). \quad (21)$$

An important feature of this solution is that it breaks the dilation symmetry of de Sitter spacetime and grows logarithmically on superhorizon scales,

$$\phi(\eta, x) \xrightarrow{ax \gg 1/H} -\beta H \left[ \ln(Hx) - \frac{1}{2(Hax)^2} + \mathcal{O}(Hax)^{-3} \right]. \quad (22)$$

At first sight, the absence of decay at large distances might be taken to signal a tension with the cosmological horizon. As we will show, however, this behavior is naturally understood in terms of the cosmological dynamics of a massless, minimally coupled scalar field. This dynamics is familiar from inflationary cosmology, where subhorizon scalar perturbations are stretched to superhorizon scales by the expansion and are amplified in the process, yielding a nearly scale-invariant spectrum of primordial scalar perturbations [20]. The same mechanism underlies the superhorizon scalar profile sourced by the point charge.

**Spectrum.** Because the scalar equation of motion is linear, the homogeneous contribution induced by the Gauss–Bonnet coupling can be separated from the part sourced by the scalar point charge. It is therefore sufficient to focus here on the latter, since the homogeneous contribution affects only the zero mode.

To see explicitly how this superhorizon behavior arises, we consider the point charge to be switched on at a finite conformal time  $\eta_0$ , at which we take  $a(\eta_0) = 1$ . The equation of motion then becomes

$$\left[ \partial_\eta^2 + 2aH\partial_\eta - \nabla^2 \right] \phi = \theta(\eta - \eta_0) \frac{4\pi\beta\delta^3(\vec{x})}{a}, \quad (23)$$

where  $\theta(z)$  is the Heaviside step function. This equation was solved in position space in [18] using the Green’s function method, yielding

$$\phi(\eta, x) = \theta(\eta - \eta_0 - x) \left[ \frac{\beta}{ax} + \beta H \ln\left(\frac{a}{1+aHx}\right) \right]. \quad (24)$$

This makes explicit that the logarithmically growing large-distance profile is established causally, rather than being present instantaneously throughout de Sitter space-time, including beyond the cosmological horizon.

A more detailed physical picture of this mechanism is obtained by examining the scalar profile in momentum space. Its Fourier transform,

$$\varphi(\eta, k) = \int d^3x e^{-i\vec{k}\cdot\vec{x}} \phi(\eta, \vec{x}), \quad (25)$$

depends only on  $k = \|\vec{k}\|$  owing to spherical symmetry, and satisfies

$$\varphi'' + 2aH\varphi' + k^2\varphi = \theta(\eta - \eta_0) \frac{4\pi\beta}{a}, \quad (26)$$

with primes denoting derivatives with respect to conformal time.

The solution satisfying the initial conditions  $\varphi(\eta_0, k) = 0$  and  $\varphi'(\eta_0, k) = 0$ , which correspond to the instantaneous switching on of the source, is obtained analytically as

$$\begin{aligned} \varphi(\eta, k) = & \frac{4\pi\beta H}{k^3} \left\{ \frac{k}{Ha} - \left[ \cos\left(\frac{k}{aH}\right) + \frac{k}{aH} \sin\left(\frac{k}{aH}\right) \right] \right. \\ & \times \left[ \sin\left(\frac{k}{H}\right) - \text{Si}\left(\frac{k}{H}\right) + \text{Si}\left(\frac{k}{Ha}\right) \right] \\ & + \left[ \sin\left(\frac{k}{aH}\right) - \frac{k}{aH} \cos\left(\frac{k}{aH}\right) \right] \\ & \left. \times \left[ \cos\left(\frac{k}{H}\right) - \text{Ci}\left(\frac{k}{H}\right) + \text{Ci}\left(\frac{k}{Ha}\right) \right] \right\}, \quad (27) \end{aligned}$$

where the sine- and cosine-integral functions are defined by  $\text{Si}(x) = \int_0^x dy \sin(y)/y$  and  $\text{Ci}(x) = -\int_x^\infty dy \cos(y)/y$ . The late-time limit of the solution takes the particularly simple form

$$\varphi(\eta, k) \xrightarrow{a \rightarrow \infty} \frac{4\pi\beta H}{k^3} \left[ \text{Si}\left(\frac{k}{H}\right) - \sin\left(\frac{k}{H}\right) \right], \quad (28)$$

and the corresponding spectrum is shown in Fig. 2, together with spectra obtained for slower switching-on of the source.

This spectrum makes the physical picture particularly clear. Only those modes that were subhorizon when the

<sup>1</sup> The scalar charge  $\lambda$  used in [18] is related to the one we use here as  $\lambda = -4\pi\beta$ .

<sup>2</sup> For clarity, Refs. [18, 21] concern a minimally coupled massless scalar field sourced by a point charge in de Sitter spacetime (and quantum-gravitational corrections to its evolution), rather than the Brans–Dicke theory as stated in [14, 22].

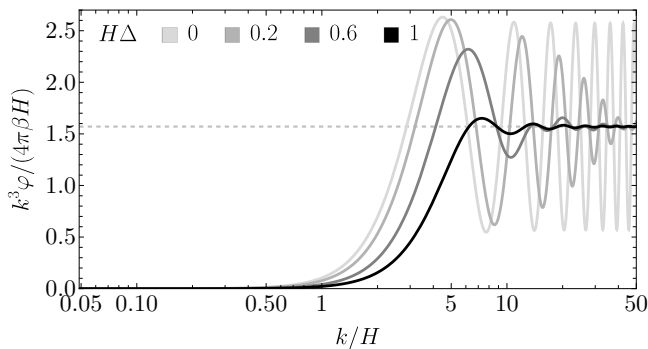


**Fig. 2.** Late-time spectra of the scalar field sourced by a point charge in de Sitter spacetime, for source profiles whose switching on begins at conformal time  $\eta_0$ , at which  $a(\eta_0) = 1$ . The curve with  $\Delta = 0$  corresponds to the instantaneous switching on described by Eq. (23). The other three curves correspond to a finite switching-on interval, implemented by replacing the step function in (23) according to  $\theta(\eta - \eta_0) \rightarrow \Theta[(\eta - \eta_0)/\Delta]$ , where  $\Theta(z)$  is taken to be the *smoothstep* function,  $\Theta(z) \equiv \theta(z)[1 - \theta(1 - z)(1 + 2z)(1 - z)^2]$ . The parameter  $\Delta$  sets the switching-on duration. Only modes that were subhorizon when the source was switched on,  $k/H > 1$ , become populated on superhorizon scales. The oscillations superimposed on the scale-invariant part of the spectrum are a consequence of abrupt switching and are smoothed out when the source is turned on more gradually.

source was switched on, namely  $k > H$ , become populated. By contrast, modes that were already superhorizon at that time, namely  $k < H$ , remain unpopulated. The point source therefore first seeds scalar perturbations on subhorizon scales, after which cosmological evolution takes over: the modes are stretched to superhorizon scales and amplified in the familiar way for a massless, minimally coupled scalar field. The result is a scale-invariant spectrum on superhorizon scales. This supports the interpretation that the superhorizon scalar profile is a consequence of cosmological scalar-field dynamics rather than of any detailed properties of the stationary, spherically symmetric source.

**Painlevé–Gullstrand coordinates.** For later comparison with the Schwarzschild–de Sitter case, it is useful to rewrite the point-source solution in Painlevé–Gullstrand coordinates [19]. These are obtained by adopting the physical distance as the radial coordinate,  $r = ax$ , and the physical time defined by  $dt = ad\eta$ . The line element then reads

$$ds^2 = -dt^2 + (dr - Hrdt)^2 + r^2 d\Omega^2. \quad (29)$$

Since the scalar field is a spacetime scalar, its profile in these coordinates is obtained by rewriting the previous solution as

$$\Phi(t, r) = (8\alpha H + \beta)H^2 t - \beta H \ln(1 + Hr) + \frac{\beta}{r}. \quad (30)$$

At superhorizon distances,

$$\Phi(t, r) \xrightarrow{r \gg 1/H} (8\alpha H + \beta)H^2 t - \beta H \ln(Hr), \quad (31)$$

it grows logarithmically with physical distance and linearly in time. This is the same large-distance behavior that will later be recovered for the Schwarzschild–de Sitter spacetime.

The scalar kinetic term, however, depends only on the radial coordinate,

$$X = \frac{H^4}{2} \left[ 64\alpha^2 H^2 - \frac{16\alpha\beta H}{Hr(1+Hr)} - \frac{\beta^2(1+H^2 r^2)}{H^4 r^4} \right]. \quad (32)$$

Although the scalar profile itself grows on superhorizon scales, the scalar kinetic term controlling the energy-momentum tensor remains much better behaved,

$$X \xrightarrow{r \gg 1/H} \frac{H^4}{2} \left[ 64\alpha^2 H^2 - \frac{\beta(16\alpha H + \beta)}{H^2 r^2} \right]. \quad (33)$$

In particular, it asymptotes to a constant, with deviations falling off as the inverse square of the physical distance.

**Backreaction.** The scalar profile (31) grows logarithmically with physical distance on superhorizon scales, in addition to growing linearly in cosmological time. This, however, does not by itself imply large backreaction or an inconsistency of the de Sitter background.

Backreaction is controlled not by the scalar profile itself, but by the energy-momentum tensor, whose source-dependent part decreases with distance. The logarithmic growth of the scalar profile is therefore not, by itself, evidence for a breakdown of the test-field approximation. This can be made explicit by comparing the Kretschmann invariant, which is constant in de Sitter,  $\mathcal{K} = 24H^4$ , to the trace of the energy-momentum tensor,

$$\mathcal{T} = H^4 \left[ 640\alpha^2 H^2 - \frac{16\alpha\beta H}{Hr(1+Hr)} - \frac{\beta^2(1+H^2 r^2)}{H^4 r^4} \right]. \quad (34)$$

The three terms in (34) have distinct origins: the first arises from the coupling to the Gauss–Bonnet term of the de Sitter background, the third from the scalar point source, and the middle term is the cross-term between the two.

The corresponding invariant backreaction diagnostic is

$$b = \frac{\beta^2 H^2}{2\sqrt{6}M_{\text{p}}^2} \left[ 640 \left( \frac{\alpha H}{\beta} \right)^2 - \frac{16(\alpha H/\beta)}{Hr(1+Hr)} - \frac{1+H^2 r^2}{H^4 r^4} \right]. \quad (35)$$

Its behavior is shown in Fig. 3. Near the source, that is on subhorizon scales,

$$b \xrightarrow{r \ll 1/H} \frac{\beta^2 H^2}{2\sqrt{6}M_{\text{p}}^2} \left[ \frac{1}{H^4 r^4} + \frac{1}{H^2 r^2} \right], \quad (36)$$

so the source-induced contribution grows rapidly as the source is approached. By contrast, on superhorizon scales,

$$b \xrightarrow{r \gg 1/H} \frac{\beta^2 H^2}{2\sqrt{6}M_{\text{p}}^2} \left[ 640 \left( \frac{\alpha H}{\beta} \right)^2 - \frac{16(\alpha H/\beta) + 1}{H^2 r^2} \right]. \quad (37)$$

Thus, even though the scalar profile itself grows logarithmically at large distances, the source-dependent part of the backreaction becomes weaker with increasing distance.

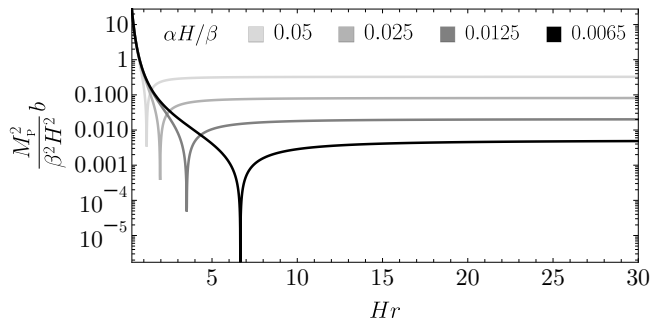


**Fig. 3.** Strength of the backreaction induced by a point scalar charge on the de Sitter background. The source-induced backreaction is strongest on subhorizon scales and decreases with distance, even though the scalar profile itself grows on superhorizon scales.

An important consequence is that if the source-induced backreaction became appreciable on cosmological scales, then it would necessarily have been much larger on subhorizon scales. The first breakdown of the test-field approximation therefore occurs near the source rather than as a cosmological-scale obstruction, and must be understood there before drawing conclusions about cosmological scales.

**Scalar radiation.** A point scalar charge in de Sitter spacetime also carries a nonvanishing radial energy flux, naturally interpreted as monopole scalar radiation [16]. To exhibit this explicitly, it is convenient to rewrite the point-source solution in static coordinates. These are related to the conformal cosmological coordinates by

$$\tau = -\frac{1}{H} \ln \left[ \frac{\sqrt{1 - H^2 a^2(\eta) x^2}}{a(\eta)} \right], \quad r = a(\eta)x, \quad (38)$$

so that the line element becomes

$$ds^2 = -h(r)d\tau^2 + \frac{dr^2}{h(r)} + r^2 d\Omega^2, \quad (39)$$

where  $h(r) = 1 - H^2 r^2$ . These coordinates cover only the static patch, that is, the region inside the cosmological horizon  $r < 1/H$ , where the time direction corresponds to the Killing vector. This makes these coordinates well suited for describing the associated stationary energy flux.

The total inward energy flux through a sphere of radius  $r$  is defined by  $\dot{M} = 4\pi r^2 T^r_{\tau}$ . To evaluate it, we rewrite the scalar profile (19) in static coordinates,

$$\begin{aligned} \Phi(\tau, r) &= (8\alpha H + \beta)H^2 \tau + 4\alpha H^2 \ln(1 - H^2 r^2) \\ &\quad + \beta H \ln \left[ \frac{\sqrt{1 - H^2 r^2}}{1 + Hr} \right] + \frac{\beta}{r}. \end{aligned} \quad (40)$$

The profile is singular at the cosmological horizon in these coordinates, but this is only an artifact of the static patch. A direct computation then gives the constant negative flux

$$\dot{M} = -4\pi\beta(\beta + 8\alpha H)H^2. \quad (41)$$

This is a purely de Sitter effect,<sup>3</sup> which vanishes in the flat-space limit  $H \rightarrow 0$ . In static coordinates, it describes a stationary outward energy flux and admits the natural interpretation of monopole scalar radiation, as discussed in Ref. [16]; see also [23, 24].

This effect suggests that the point source cannot support the same stationary scalar profile indefinitely. The outward flux indicates that the system must eventually evolve beyond the test-field description, as the source radiates away its entire mass [16]. However, the detailed late-time fate of the source and of the scalar profile it supports is not yet fully understood [17].

## V. SCHWARZSCHILD-DE SITTER SPACETIME

We now turn to the Schwarzschild-de Sitter spacetime, which combines the local black-hole structure of the Schwarzschild solution with the large-scale cosmological structure of de Sitter space. This is the geometry in which the two mechanisms isolated in the previous sections coexist and can be studied together.

The Schwarzschild-de Sitter line element in Kottler coordinates is

$$ds^2 = -F(r)d\tau^2 + \frac{dr^2}{F(r)} + r^2 d\Omega^2, \quad (42)$$

where  $F(r) = 1 - r_s/r - H^2 r^2$ . The black-hole horizon and the cosmological horizon, respectively, are located at

$$r_{\text{BH}} = \frac{2}{\sqrt{3}H} \sin \left[ \frac{1}{3} \arcsin \left( \frac{3\sqrt{3}}{2} H r_s \right) \right], \quad (43)$$

$$r_{\text{C}} = \frac{1}{H} \cos \left[ \frac{1}{3} \arcsin \left( \frac{3\sqrt{3}}{2} H r_s \right) \right] - \frac{r_{\text{BH}}}{2}. \quad (44)$$

We focus on the regime in which the black-hole and cosmological horizons are widely separated, so that  $H r_s \ll 1$ . In this limit, the horizon radii are well approximated by the parameters appearing in the line element,

$$r_{\text{BH}} = r_s \left[ 1 + (H r_s)^2 + \mathcal{O}(H r_s)^4 \right], \quad (45)$$

$$r_{\text{C}} = \frac{1}{H} \left[ 1 - \frac{1}{2} H r_s - \frac{3}{8} (H r_s)^2 + \mathcal{O}(H r_s)^3 \right]. \quad (46)$$

<sup>3</sup> While this effect of scalar monopole radiation is not observed in flat space in 3+1 dimensions, it is found in lower 2+1 and 1+1 dimensions [25].

**Integrating equation of motion.** Following the static-coordinate strategy of [14], we adopt the ansatz

$$\Phi(\tau, r) = \mathcal{Q}H^2\tau + \varphi(r), \quad (47)$$

where the first term is a homogeneous solution, while the radial function  $\varphi(r)$  captures the part sourced by the Gauss–Bonnet invariant,  $\mathcal{G} = 24H^4 + 12r_s^2/r^6$ . The equation of motion then reduces to

$$\partial_r \left( r^2 F(r) \partial_r \varphi \right) = -\alpha \left( \frac{12r_s^2}{r^4} + 24H^4 r^2 \right), \quad (48)$$

The equation can then be integrated once, yielding

$$\partial_r \varphi = \frac{1}{r^2 F(r)} \left( 4\alpha F'(r) [1 - F(r)] - \mathcal{C} \right), \quad (49)$$

where  $\mathcal{C}$  is an integration constant. A second integration would produce only an additive constant in the scalar field, which is physically irrelevant because of shift symmetry.

The two physically relevant constants are therefore  $\mathcal{Q}$  and  $\mathcal{C}$ . They are constrained by requiring finiteness of the scalar kinetic term,

$$X = \frac{\mathcal{Q}^2 H^4}{2F(r)} - \frac{1}{2r^4 F(r)} \left( 4\alpha F'(r) [1 - F(r)] - \mathcal{C} \right)^2, \quad (50)$$

at the two horizons. Demanding regularity at the black-hole horizon (45) and at the cosmological horizon (46) yields, respectively,

$$(Hr_{\text{BH}})^4 \mathcal{Q}^2 = [4\alpha F'(r_{\text{BH}}) - \mathcal{C}]^2, \quad (51)$$

$$(Hr_c)^4 \mathcal{Q}^2 = [4\alpha F'(r_c) - \mathcal{C}]^2. \quad (52)$$

At this stage, however, these conditions still admit four algebraic branches,

$$\mathcal{C} = 4\alpha \frac{r_c^2 F'(r_{\text{BH}}) \mp r_{\text{BH}}^2 F'(r_c)}{r_c^2 \mp r_{\text{BH}}^2}, \quad (53)$$

$$|\mathcal{Q}| = 4\alpha \frac{F'(r_{\text{BH}}) - F'(r_c)}{H^2(r_c^2 \mp r_{\text{BH}}^2)}. \quad (54)$$

This branch ambiguity is not most naturally resolved in Kottler coordinates, since they are singular at the cosmological horizon, just as static coordinates are in pure de Sitter space. The behavior of the scalar profile across the horizons, and hence the selection of the appropriate branch, are more naturally analyzed in coordinates that remain regular at both horizons. We now turn to such a description.

**Painlevé–Gullstrand coordinates.** A horizon-regular representation of the Schwarzschild–de Sitter spacetime is given by Painlevé–Gullstrand coordinates [19]. The transformation  $\tau = t + w(r)$ , with

$$w(r) = \int \frac{dr}{F(r)} \sqrt{1 - F(r)} \quad (55)$$

brings the line element to the form

$$ds^2 = -dt^2 + \left( dr - \sqrt{1 - F(r)} dt \right)^2 + r^2 d\Omega^2. \quad (56)$$

It reduces to the Schwarzschild line element in Painlevé–Gullstrand form (13) in the limit  $H \rightarrow 0$ , and to the de Sitter line element in Painlevé–Gullstrand form (29) in the limit  $r_s \rightarrow 0$ .

The full scalar profile in these coordinates reads

$$\Phi(t, r) = \mathcal{Q}H^2 t + \mathcal{Q}H^2 w(r) + \varphi(r). \quad (57)$$

It is more convenient, however, to consider the radial derivative of the scalar profile and demand its continuity across the horizons:

$$\partial_r \Phi(t, r) = \frac{H^2 r^2 \mathcal{Q} \sqrt{1 - F(r)} + 4\alpha F'(r) [1 - F(r)] - \mathcal{C}}{r^2 F(r)}. \quad (58)$$

This yields two linear conditions on the parameters,

$$(Hr_{\text{BH}})^2 \mathcal{Q} = \mathcal{C} - 4\alpha F'(r_{\text{BH}}), \quad (59)$$

$$(Hr_c)^2 \mathcal{Q} = \mathcal{C} - 4\alpha F'(r_c), \quad (60)$$

and these conditions uniquely determine  $\mathcal{Q}$  and  $\mathcal{C}$ ,

$$\mathcal{Q} = 4\alpha \frac{F'(r_{\text{BH}}) - F'(r_c)}{H^2(r_c^2 - r_{\text{BH}}^2)}, \quad (61)$$

$$\mathcal{C} = 4\alpha \frac{r_c^2 F'(r_{\text{BH}}) - r_{\text{BH}}^2 F'(r_c)}{r_c^2 - r_{\text{BH}}^2}. \quad (62)$$

This is the value for the constants obtained in [14] in the static coordinates, where the degeneracy can be broken by appealing to the finiteness of the shift-charge current, which comes with its own subtleties [26]. In the limit  $Hr_s \ll 1$  that we are working in, these two constants are the same, up to small corrections,  $\mathcal{Q} = 4\alpha/r_s [1 + \mathcal{O}(Hr_s)] = \mathcal{C}$ .

With this choice, the radial derivative of the scalar field is continuous across both horizons. Although Eq. (58) can be integrated explicitly, the resulting expression is cumbersome and will not be needed here. On superhorizon scales, the derivative simplifies to

$$\partial_r \Phi(t, r) \xrightarrow{r \gg r_c} \frac{H}{r} (8\alpha H - \mathcal{Q}), \quad (63)$$

which integrates straightforwardly to

$$\Phi(t, r) \xrightarrow{r \gg r_c} \mathcal{Q}H^2 t + (8\alpha H - \mathcal{Q})H \ln(Hr). \quad (64)$$

This has precisely the same structure as the superhorizon behavior of the de Sitter point-source profile (31), upon identifying the effective source strength as  $\beta = \mathcal{Q} - 8\alpha H \approx \mathcal{C}$ . This agreement shows that the black hole sources the same superhorizon scalar profile as a point source in de Sitter, with an amplitude fixed by the local black-hole physics.

This result supports the interpretation of the scalar-hair tail in terms of the physical mechanism outlined in Sec. IV. The black hole perturbs the scalar field locally, after which its superhorizon evolution is governed by the cosmological dynamics of a massless, minimally coupled scalar field.

**Backreaction.** We evaluate the invariant backreaction diagnostic by comparing the Kretschmann invariant,

$$\mathcal{K} = \frac{12r_s^2}{r^6} + 24H^4 = \mathcal{G}, \quad (65)$$

to the trace of the energy-momentum tensor,

$$\mathcal{T} = 2X + 24\alpha^2 H^2 \mathcal{G}. \quad (66)$$

Its radial dependence is shown in Fig. 4.

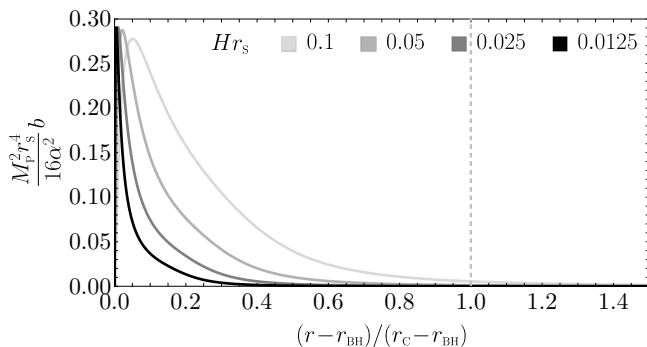


**Fig. 4.** Strength of the backreaction of the scalar field on the Schwarzschild–de Sitter background. Backreaction first becomes important on subhorizon scales, close to the black hole, and decreases substantially before the cosmological horizon.

In the regime where

$$\left(\frac{4\alpha}{r_s}\right)^2 \ll (M_P r_s)^2, \quad (67)$$

the backreaction can be neglected everywhere, both on subhorizon and superhorizon scales, and the test-field approximation provides a good description of the scalar hair. When the hierarchy (67) is not satisfied, backreaction must instead be taken into account. As is clear from Fig. 4, it becomes important first on subhorizon scales. Thus, the first breakdown of the test-field approximation occurs near the black hole, while the superhorizon regime remains under control. This indicates that the relevant nonlinear problem is localized and should be resolved there before drawing conclusions about the cosmological-scale profile.

**Scalar monopole radiation.** The parallel between the Schwarzschild–de Sitter spacetime and the point source in de Sitter extends also to scalar monopole radiation. In the region between the two horizons, Kottler coordinates provide a natural framework for describing the associated stationary energy flux.

The total energy inflow through a sphere of radius  $r$  is again given by  $\dot{M} = 4\pi r^2 T^r_r$ . Computing this for our system gives the constant result <sup>4</sup>

$$\dot{M} = -4\pi \mathcal{C} \mathcal{Q} H^2, \quad (68)$$

where again the negative sign indicates an outward energy flux. Up to small corrections of order  $\mathcal{O}(Hr_s)$ , this result matches the one obtained for the point scalar source in de Sitter (41), upon the same identification of parameters,  $\beta = \mathcal{Q} - 8\alpha H \approx \mathcal{C}$ , used above to match the asymptotic superhorizon scalar profiles.

This result is consistent with the behavior of a scalar point charge in de Sitter spacetime, where the outward flux is interpreted as monopole scalar radiation. The Schwarzschild–de Sitter solution therefore admits the same interpretation: the time-dependent scalar configuration carries a steady outward energy flux. In this sense, the superhorizon scalar hair cannot be sustained indefinitely with an arbitrarily large energy content, since the associated flux is constrained by the finite mass of the black hole.

For the test-field approximation to remain applicable, the black hole should not evolve appreciably during a Hubble time, namely  $|\dot{M}|/H \ll M$ . This condition is equivalent to

$$\left(\frac{4\alpha}{r_s}\right)^2 \ll \frac{(M_P r_s)^2}{H r_s}. \quad (69)$$

Because we assume  $Hr_s \ll 1$ , this condition is weaker than the one obtained for the absence of backreaction in (67). The energy flux therefore does not set the leading limitation on the test-field approximation: by the time it would become relevant, scalar backreaction would already have become important. This mirrors the asymptotically flat case, where the energy flux is absent but the backreaction due to scalar hair can nevertheless become appreciable.

This does not alter our main conclusion about the regime of validity of the test-field approximation. As the black hole presumably slowly loses mass, the system is driven toward the regime in which local scalar backreaction becomes important. Thus, long before the ultimate late-time evolution could be inferred from the test-field solution alone, the perturbative treatment would already cease to be trustworthy near the black hole. Whether this would terminate the scalar monopole radiation or not remains an open question.

## VI. DISCUSSION

The results presented here show that the logarithmically growing scalar-hair profile on cosmological scales

<sup>4</sup> This computation is facilitated by *Cadabra* [27–29].

in the linearly coupled shift-symmetric scalar–Gauss–Bonnet theory should not be interpreted as an inconsistency of the solution or as an obstruction associated with the cosmological horizon. Rather, it is the expected large-distance behavior of a massless, minimally coupled scalar field sourced by a localized object in an expanding de Sitter background. In this respect, the cosmological profile is not a special feature of black holes, but a manifestation of the underlying scalar-field dynamics.

This conclusion is clarified by comparing the three systems studied in this work. The Schwarzschild analysis isolates the local scalarization mechanism that fixes the effective scalar charge of the black hole on subhorizon scales. The point-source solution in de Sitter then isolates the cosmological evolution of a localized scalar charge and makes the origin of the logarithmic superhorizon profile transparent.

Finally, the Schwarzschild–de Sitter solution shows that these two elements coexist in a single geometry: once the scalar field is described in coordinates that remain regular across both the black-hole and cosmological horizons, the black hole reproduces the same asymptotic structure as the de Sitter point source. In this sense, the asymptotic scalar profile of the black hole is the cosmological continuation of locally sourced scalar hair.

The parallel between the Schwarzschild–de Sitter case and the point source in de Sitter can be understood directly from the scalar equation of motion. In both cases, the scalar field behaves as a massless, minimally coupled field sourced by an effective localized charge: in one case this charge is provided explicitly by a point source, while in the other it is induced by the geometry through the Gauss–Bonnet invariant. The latter may be viewed heuristically as a superposition of point sources spread through the localized subhorizon region. From the point of view of the superhorizon scalar profile, this distinction is largely irrelevant: once the local source fixes the total scalar charge, the subsequent large-distance evolution is governed by the same cosmological dynamics.

A related lesson is methodological. The Schwarzschild–de Sitter problem is most naturally analyzed in Painlevé–Gullstrand coordinates, which remain regular at both horizons. In these coordinates the physically relevant branch is selected unambiguously by demanding continuity of the radial derivative of the scalar profile across the two horizons, and the resulting superhorizon behavior can be read off directly. This is important because Kottler coordinates, used in earlier analyses, cover only the static patch and it is not immediately clear how the scalar hair profile extends beyond it. The coordinates that we employ, on the other hand, make clear what the long-distance behavior of the scalar profile is and how it connects to the analogous scalar profile sourced by point scalar charges.

The point-source analysis also provides a simple physical picture for the origin of the cosmological profile. A localized source first excites scalar perturbations on subhorizon scales. Cosmological expansion then stretches

those perturbations to superhorizon scales and amplifies them in the familiar way for a massless, minimally coupled scalar field. The momentum-space spectrum in Fig. 2 makes this mechanism particularly clear: only modes that were initially subhorizon become populated, and their subsequent evolution gives rise to a scale-invariant superhorizon spectrum. The same mechanism controls the superhorizon profile of the black-hole solution, while the local black-hole physics enters only through the effective scalar charge that fixes its overall amplitude.

Our backreaction analysis supports the same interpretation. In all examples studied here, the first regime in which the test-field approximation is expected to fail occurs on subhorizon scales, near the localized source, rather than on cosmological scales. The dominant nonlinear problem is therefore not the existence of the logarithmic profile itself, but the behavior of the scalar configuration in the vicinity of the black hole. If backreaction becomes important, its primary effect should be to modify the effective local source that feeds the cosmological profile, rather than to eliminate the large-distance behavior generated by cosmological evolution.

Perhaps the most striking ingredient emerging from the analysis is the presence of a steady outward energy flux associated with the time-dependent scalar configuration. This occurs already for a point scalar charge in de Sitter spacetime, where it is naturally interpreted as monopole scalar radiation. The Schwarzschild–de Sitter solution exhibits the same effect up to small corrections in  $Hr_s$ .

Even though this flux does not set the leading limitation on the test-field approximation in the regime  $Hr_s \ll 1$ , it does provide a new physical picture of the system where the scalarized black hole is embedded in de Sitter space asymptotically. Even though the energy-momentum tensor of such a configuration is static, it encodes an outward energy flux that prevents the system from being considered stationary. This flux signals that the scalarized black hole embedded in cosmology does not necessarily have to resemble the scalarized black hole with flat asymptotics. The outward flux seems to push the black hole towards smaller Schwarzschild radii, bringing it steadily closer to the regime where backreaction becomes important.

Although self-consistent cosmological solutions have not been constructed here, the test-field results strongly suggest that the cosmological-scale profile should persist even when the near-source region becomes nonlinear. A fully nonlinear black-hole configuration may differ substantially from the perturbative solution near the horizon, but as long as it remains a localized source of scalar charge, its effect at large distances should still be governed by the same cosmological mechanism identified in this work. This also clarifies why earlier attempts to construct self-consistent black-hole solutions with de Sitter asymptotics under the assumption of a static scalar profile encounter difficulty: the cosmological dynamics of a massless, minimally coupled scalar field generically in-

roduces time dependence into the scalar hair, together with an associated energy flux. Currently it is not clear whether the black hole keeps radiating scalar monopole radiation indefinitely, or whether there is an equilibrium end point to this process where the scalar charged is somehow screened. It is also interesting to note that modifications of the scalar kinetic term can turn the cosmological hair from secondary to primary [30], though it is not completely clear to which degree this distinction applies to situations where hair is not stationary.

## ACKNOWLEDGMENTS

We are indebted to Ignacy Sawicki for discussions on the subject, and for the critical reading of the manuscript. We also thank José Luis Blázquez-Salcedo and Alexander Vikman for useful comments. DG was supported by the Czech Science Foundation (GAČR) grant 24-13079S. DJG acknowledges support from the Comunidad de Madrid under predoctoral contract PIPF-2023/TEC-29931, and thanks FZU's Department of Cosmology and Gravitational Physics for their kind hospitality.

- 
- [1] J. D. Bekenstein, “Novel “no-scalar-hair” theorem for black holes,” *Phys. Rev. D* **51** (1995) no.12, R6608
- [2] L. Hui and A. Nicolis, “No-Hair Theorem for the Galileon,” *Phys. Rev. Lett.* **110** (2013), 241104 [arXiv:1202.1296 [hep-th]].
- [3] T. P. Sotiriou and S. Y. Zhou, “Black hole hair in generalized scalar-tensor gravity,” *Phys. Rev. Lett.* **112** (2014), 251102 [arXiv:1312.3622 [gr-qc]].
- [4] G. Antoniou, A. Bakopoulos and P. Kanti, “Evasion of No-Hair Theorems and Novel Black-Hole Solutions in Gauss-Bonnet Theories,” *Phys. Rev. Lett.* **120** (2018) no.13, 131102 [arXiv:1711.03390 [hep-th]].
- [5] T. P. Sotiriou and S. Y. Zhou, “Black hole hair in generalized scalar-tensor gravity: An explicit example,” *Phys. Rev. D* **90** (2014), 124063 [arXiv:1408.1698 [gr-qc]].
- [6] S. R. Coleman, J. Preskill and F. Wilczek, “Growing hair on black holes,” *Phys. Rev. Lett.* **67** (1991), 1975-1978
- [7] S. R. Coleman, J. Preskill and F. Wilczek, “Quantum hair on black holes,” *Nucl. Phys. B* **378** (1992), 175-246 [arXiv:hep-th/9201059 [hep-th]].
- [8] H. Ogawa, T. Kobayashi and T. Suyama, “Instability of hairy black holes in shift-symmetric Horndeski theories,” *Phys. Rev. D* **93** (2016) no.6, 064078 [arXiv:1510.07400 [gr-qc]].
- [9] R. Benkel, T. P. Sotiriou and H. Witek, “Black hole hair formation in shift-symmetric generalised scalar-tensor gravity,” *Class. Quant. Grav.* **34** (2017) no.6, 064001 [arXiv:1610.09168 [gr-qc]].
- [10] J. F. M. Delgado, C. A. R. Herdeiro and E. Radu, “Spinning black holes in shift-symmetric Horndeski theory,” *JHEP* **04** (2020), 180 [arXiv:2002.05012 [gr-qc]].
- [11] Y. Brihaye, B. Hartmann and J. Urrestilla, “Solitons and black hole in shift symmetric scalar-tensor gravity with cosmological constant,” *JHEP* **06** (2018), 074 [arXiv:1712.02458 [gr-qc]].
- [12] A. Bakopoulos, G. Antoniou and P. Kanti, “Novel Black-Hole Solutions in Einstein-Scalar-Gauss-Bonnet Theories with a Cosmological Constant,” *Phys. Rev. D* **99** (2019) no.6, 064003 [arXiv:1812.06941 [hep-th]].
- [13] Y. Brihaye, C. Herdeiro and E. Radu, “Black Hole Spontaneous Scalarisation with a Positive Cosmological Constant,” *Phys. Lett. B* **802** (2020), 135269 [arXiv:1910.05286 [gr-qc]].
- [14] E. Babichev, I. Sawicki and L. G. Trombetta, “Black-hole hair in scalar-Gauss-Bonnet gravity is altered by cosmology,” *Phys. Rev. D* **111** (2025) no.4, L041502 [arXiv:2403.15537 [gr-qc]].
- [15] L. Parker, “Particle creation in expanding universes,” *Phys. Rev. Lett.* **21** (1968), 562-564
- [16] L. M. Burko, A. I. Harte and E. Poisson, “Mass loss by a scalar charge in an expanding universe,” *Phys. Rev. D* **65** (2002), 124006 [arXiv:gr-qc/0201020 [gr-qc]].
- [17] E. T. Akhmedov, A. Roura and A. Sadofyev, “Classical radiation by free-falling charges in de Sitter spacetime,” *Phys. Rev. D* **82** (2010), 044035 [arXiv:1006.3274 [gr-qc]].
- [18] D. Glavan, S. P. Miao, T. Prokopec and R. P. Woodard, “Breaking of scaling symmetry by massless scalar on de Sitter,” *Phys. Lett. B* **798** (2019), 134944 [arXiv:1908.11113 [gr-qc]].
- [19] R. Gaur and M. Visser, “Cosmology in Painlevé-Gullstrand coordinates,” *JCAP* **09** (2022), 030 [arXiv:2207.08375 [gr-qc]].
- [20] Y. Akrami *et al.* [Planck], “Planck 2018 results. X. Constraints on inflation,” *Astron. Astrophys.* **641** (2020), A10 [arXiv:1807.06211 [astro-ph.CO]].
- [21] D. Glavan, S. P. Miao, T. Prokopec and R. P. Woodard, “Large logarithms from quantum gravitational corrections to a massless, minimally coupled scalar on de Sitter,” *JHEP* **03** (2022), 088 [arXiv:2112.00959 [gr-qc]].
- [22] E. Babichev, G. Esposito-Farèse, I. Sawicki and L. G. Trombetta, “Large black-hole scalar charges induced by cosmology in Horndeski theories,” *Phys. Rev. D* **112** (2025) no.2, 024043 [arXiv:2504.07882 [gr-qc]].
- [23] T. C. Quinn, “Axiomatic approach to radiation reaction of scalar point particles in curved space-time,” *Phys. Rev. D* **62** (2000), 064029 [arXiv:gr-qc/0005030 [gr-qc]].
- [24] E. Poisson, “The Motion of point particles in curved space-time,” *Living Rev. Rel.* **7** (2004), 6 [arXiv:gr-qc/0306052 [gr-qc]].
- [25] L. M. Burko, “Instability of scalar charges in (1+1)-dimensions and (2+1)-dimensions,” *Class. Quant. Grav.* **19** (2002), 3745-3752 [arXiv:gr-qc/0201021 [gr-qc]].
- [26] P. Creminelli, N. Loayza, F. Serra, E. Trincherini and L. G. Trombetta, “Hairy Black-holes in Shift-symmetric Theories,” *JHEP* **08** (2020), 045 [arXiv:2004.02893 [hep-th]].
- [27] K. Peeters, “Introducing Cadabra: A Symbolic computer algebra system for field theory problems,” [arXiv:hep-th/0701238 [hep-th]].
- [28] K. Peeters, “A Field-theory motivated approach to symbolic computer algebra,” *Comput. Phys. Commun.* **176** (2007), 550-558 [arXiv:cs/0608005 [cs.SC]].
- [29] K. Peeters, “Cadabra2: computer algebra for field theory revisited,” *J. Open Source Softw.* **3** (2018) no.32, 1118
- [30] G. Lara, G. Trenkler and L. G. Trombetta, “Primary black-hole scalar charges and kinetic screening in  $K$ -essence-Gauss-Bonnet gravity,” [arXiv:2512.23683 [gr-qc]].